IEICE TRANSACTIONS

on Communications

DOI:10.1587/transcom.2019OBI0001

Publicized:2020/06/08

This advance publication article will be replaced by the finalized version after proofreading.

A PUBLICATION OF THE COMMUNICATIONS SOCIETY

The Institute of Electronics, Information and Communication Engineers

Kikai-Shinko-Kaikan Bldg., 5-8, Shibakoen 3chome, Minato-ku, TOKYO, 105-0011 JAPAN

INVITED PAPER

Ultra-Low Crosstalk Multi-core Fiber with Standard 125-μm Cladding Diameter for 10,000 km-class Long-haul Transmission

Yuto SAGAE[†], ***Member,*** **Takashi MATSUI**[†], ***Member,*** **Taiji SAKAMOTO**[†], ***Member,*** **and Kazuhide NAKAJIMA**[†], ***Member***

SUMMARY
We propose an ultra-low inter-core crosstalk (XT) multi-core fiber (MCF) with standard 125-μm cladding. We show the fiber design and fabrication results of an MCF housing four cores with W-shaped index profile; it offers XT of less than -67 dB/km over the whole C+L band. This enables us to realize 10,000–km transmission with negligible XT penalty. We also observe a low-loss of 0.17 dB/km (average) at a wavelength of 1.55 μm and other optical properties compatible with ITU-T G.654.B fiber. We also elucidate its good micro-bend resistance in terms of both the loss and XT to confirm its applicability to high-density optical fiber cables. Finally, we show that fabricating the MCF is feasible along with long-distance transmission by confirming the that the XT noise performance corresponds to transmission distances of 10,000 km or more.

key words: *Spatial division multiplexing, Multi-core fiber, Long-distance transmission, Micro-bending*

1. Introduction

To overcome the transmission capacity limitation of 100 Tbit/s of conventional single mode fiber (SMF) based optical networks, the space division multiplexing (SDM) technique is one of the key technologies. SDM fibers can be classified into multi-core fibers (MCFs), few-mode fibers (FMFs) and few-mode MCFs (FM-MCFs). Recently, the transmission capacity of 10.16 Pbit/s was demonstrated by utilizing a 19-core fiber with 6 modes in each core [1]. However, mode-division multiplexing transmission using FMF or FM-MCF generally needs complex multi-input and multi-output (MIMO) technologies. Single-mode MCFs can, on the other hand, be utilized without such complex MIMO signal processing if the inter-core XT is sufficiently suppressed.

In the last decade, several types of MCFs have been investigated. One is the homogeneous MCF that houses identical cores. A 22-core fiber realized an inter-core XT of about -45 dB/km with cladding diameter of 260 μm and a transmission capacity of 2.15 Pbit/s by utilizing wavelengths throughout the C+L band [2]. To increase the core density, the heterogeneous MCF was proposed [3]. Combining several types of core in one fiber dramatically suppresses the inter-core XT even with small core pitch values. 37 cores of three types were successfully set within 248.3-μm diameter cladding [4].

Recent investigations have considered the practical use of SDM techniques from the aspect of SDM fibers and cables [5-8]. One report focused on MCFs with standard 125-μm cladding diameter, which are compatible with ITU-T Recommendations G.652 or G.657, to improve fiber productivity and utilize the existing SMF-based optical equipment [5, 6]. By designing such an MCF with standard cladding, 316-km PDM-16QAM transmission at 118.5 Tbit/s was demonstrated with a view to practical transmission systems [9]. For long-distance SDM transmission, a low-loss and large-effective area two-core fiber with standard cladding was proposed; it utilizes the core structure developed for a conventional G.654.E fiber [10].

We proposed a four-core fiber (4CF) with standard 125-μm cladding; it offers ultra-low XT performance in the C+L-band [11]. The proposed fiber houses four W-shaped index cores. The fabricated 4CF realized an ultra-low inter-core XT of less than -67 dB/km at a wavelength of 1.625 μm while its optical properties complied with ITU-T G.654.B fiber. We then observed the negligible impact of lateral pressure influence on both the loss and XT. This paper investigates in detail the influence of XT noise on the transmission quality of the fabricated 4CF in quasi long-distance transmission. The results of the transmission experiments reveal that the fabricated 4CF offers the XT noise values needed to support the 25,000-km transmission of DP-QPSK signals. On the basis of these results, we can expect our fabricated 4CF to be applicable to 10,000-km class long-distance transmission systems.

2. 4CF design

Following on from our MCF with standard cladding diameter [5], we design here a 4CF, see Fig. 1(a). Long-distance transmission systems must offer low transmission loss. Accordingly, pure silica glass is used as the core medium and the W-shaped index profile shown in Fig. 1(b). The pure silica glass core reduces the Rayleigh scattering loss [12] and the W-shaped index profile realizes low macro- and micro-bending loss

†The authors are with Access Network Service Systems Labs., NTT Corporation, Tsukuba-shi, 305-0805 Japan.

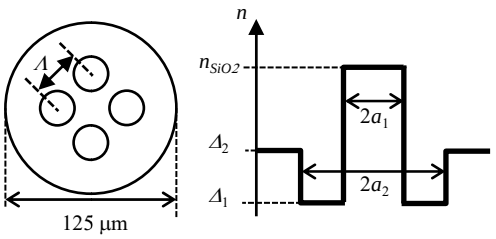

(a) (b)

Fig. 1 (a) Core allocation of the proposed fiber and (b) designed index profile

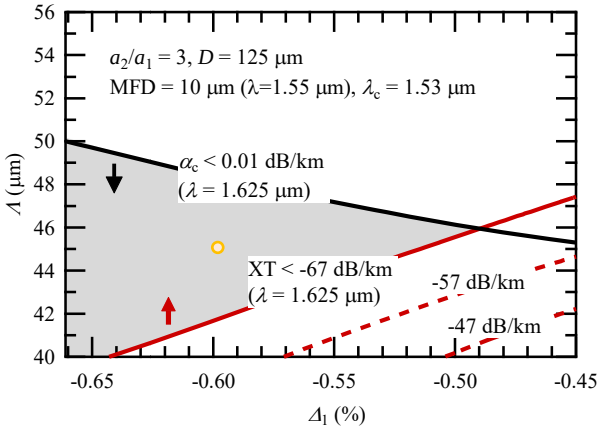

Fig. 2 Calculated values of the inter-core XT and α_c as functions of Δ_1 and Λ

owing to its strong optical confinement [13]. To ensure the other optical properties are compatible with long-distance transmission, we set the cutoff wavelength (λ_c) under 1.53 μm and the mode field diameter (MFD) larger than 10 μm, which ensures compatibility with ITU-T G.654.B fiber. The required XT at the receiver depends on the transmission formats. According to the investigation of XT penalty in Refs. [14, 15], XT below -24 dB is necessary if the OSNR penalty is to be held under 1 dB for 16QAM transmission. Because the XT noise accumulates linearly with transmission length [16], the ultra-low inter-core XT of -67 dB/km is required in for the 10,000-km transmission of 16QAM signals. Although a larger inter-core pitch (Λ) suppresses the inter-core XT as it reduces the electric field overlap between cores, such a large Λ usually triggers excess loss increase for a fixed cladding diameter. Here, we set the excess loss (α_c) below 0.01 dB/km at the wavelength of 1.625 μm.

A_{eff} is mainly determined by the core radius a_1, whereas λ_c is given by the relative index difference between the depressed layer and cladding, Δ_2. The macro-bending loss can be adequately suppressed by setting the depressed layer radius of a_2 to $3a_1$ [13]. Thus we calculated the inter-core XT and α_c as a function of the relative index difference between the core and the depressed layer, Δ_1 and Λ. Figure 2 plots the calculated values of the inter-core XT and α_c. Here a_1 and Δ_2 were

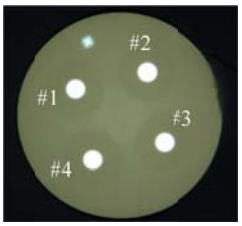

Fig. 3 Cross section of the fabricated FCF

Table 1 Designed and observed structural parameters

	Design	Fabricated FCF
D (μm)	125	124.6
Λ (μm)	45	44.7±0.2
a_2/a_1	3.0	3.0±0.1

selected so that MFD and λ_c were held to 10 μm and λ_c = 1.53 μm at each condition. The red and black solid lines correspond to the conditions realizing XT = 67 dB/km and α_c = 0.01 dB/km, respectively. The conditions realizing XT of -57 and -47 dB/km are indicated by the red broken lines. XT and α_c decrease as Δ_1 falls because the optical confinement is enhanced. We also confirmed that large Λ suppressed the XT owing to less optical-field overlap between cores. However, when the cladding diameter was 125 μm, the large Λ increased α_c because of insufficient outer-cladding thickness. The parameters lying in the shaded area satisfy our requirements and thus are assumed to realize the desired ultra-low XT 4CF with standard cladding diameter. We fabricated a batch of fiber using the design values indicated by the yellow point to evaluate the feasibility of our design.

3. Fabrication results

Figure 3 shows the cross-section of the fabricated 4CF. It sets four W-shaped silica cores in a square lattice. Table 1 summarizes the designed and observed structural parameters. Its cladding diameter D is 124.6 μm, inter-core pitch Λ is 44.7±0.2 μm and a_2/a_1 is 3.0±0.1.

First, the optical properties of each core are summarized in Table 2. The MFDs of 10.2~10.3 μm at the wavelength of 1.55 μm are compatible with those of G.654.B fiber. A_{eff} values of 86.2~88.9 μm at the wavelength of 1.55 μm are larger than intended. This seems to be because the a_1 of each core were larger than our design values. The bending loss values, α_b, at the wavelength of 1.625 μm are extremely small, less than 0.12 dB/turn, which is comparable to ITU-T G.657.B3 bending-loss insensitive fiber. This was made possible by the low-index depressed layer. The λ_c were shorter than 1.47 μm as is true for conventional cutoff shifted fibers (CSFs). Loss values at the wavelength of 1.55 μm ranged from 0.18 to 0.19 dB/km. Here the optical confinement losses were expected to be adequately suppressed as the design of Figure 2 was used. The observed chromatic dispersion values, σ, of 21.8~21.9 ps/km/nm and PMD coefficients of 0.04~0.06 at the wavelength of 1.55 μm are comparable with those of conventional CSFs. Finally, the inter-core XTs are shown as average values of XTs from adjacent cores. We confirmed that the inter-core XT was lower than -67 dB/km at the longest wavelength in

Table 2 Optical properties measured in each core and the values given in ITU-T G.654.B

	λ (μm)	#1	#2	#3	#4	G.654.B
MFD (μm)	1.55	10.2	10.2	10.2	10.3	9.5-13.0
A_{eff} (μm^2)	1.55	86.2	87.2	86.2	88.9	-
α_b (dB/turn, R=5 mm)	1.625	0.08	0.07	0.05	0.12	-
λ_c (μm)	-	1.46	1.47	1.46	1.44	<1.53
α (dB/km)	1.55	0.18	0.18	0.18	0.19	<0.22
σ (ps/km/nm)	1.55	21.8	21.8	21.8	21.9	<22
PMD coefficient (ps/√km)	1.55	0.05	0.06	0.06	0.04	<0.2
Inter-core XT (dB/km)	1.625	-70	-67	-68	-68	-

the L-band.

Figure 4(a) shows the measured loss spectra in the entire C+L-band. The red, yellow, green and blue lines correspond to the measured values of core #1, #2, #3 and #4, respectively, in the fabricated 4CF; the measured values of a commercial G.654.B fiber are shown by the black dashed line for comparison. The losses of the fabricated 4CF were slightly larger than that of G.654.B fiber. These loss differences increase in the short wavelength region. Moreover, cores #1 and #4 had slightly higher losses than the other cores. We examined the contribution of Rayleigh scattering, infrared (IR) absorption and OH absorption to analyze these loss spectra. The contribution of Rayleigh scattering was analyzed by λ^{-4} dependence of the loss as shown in Fig. 4(b). The losses of both of the fabricated 4CF and the G.654.B fiber linearly increased for λ^{-4} values of 0.5~1.0. Linear fitting deduced that cores #1, #2, #3 and #4 had slightly higher Rayleigh scattering coefficients, 0.936, 0.940, 0.938 and 0.926 dB/km/μm^4, than the G.654.B fiber, 0.900 dB/km/μm^4. The contribution of IR and OH absorption was derived by Lorentzian and exponential function fitting. Table 3 summarizes the analyzed IR and OH absorption losses at the wavelengths of 1.50 μm, 1.55 μm and 1.625 μm. IR absorption yielded no noticeable difference between the fabricated 4CF and the G.654.B fiber. On the other hand, higher contributions of OH absorption were observed at three wavelengths in the fabricated 4CF compared to the G.654.B fiber. In particular, the fabricated 4CF had remarkably different OH absorption values, 0.019, 0.010, 0.012 and 0.036

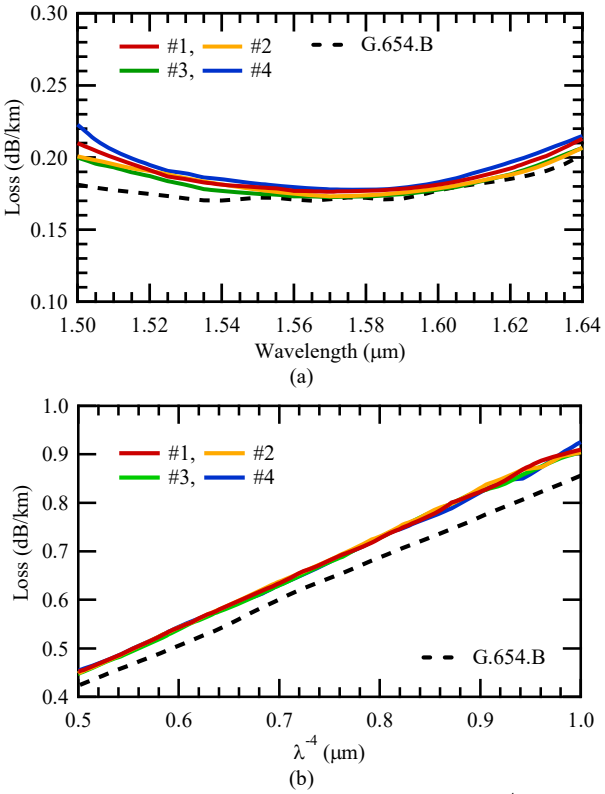

Fig. 4 Measured loss spectrum as a function of (a) λ and (b) λ^{-4}

Table 3 Results of the loss factor analysis

Loss (dB/km)	λ (μm)	#1	#2	#3	#4	G.654.B
IR absorption	1.50	0.003	0.003	0.003	0.002	0.005
	1.55	0.011	0.010	0.010	0.009	0.015
	1.625	0.058	0.054	0.054	0.053	0.060
OH absorption	1.50	0.019	0.010	0.012	0.036	0.001
	1.55	0.010	0.005	0.006	0.018	0.000
	1.625	0.005	0.003	0.003	0.009	0.000

dB/km, at the wavelength of 1.50 μm, from the G.654.B fiber. Moreover, at the wavelengths of 1.55 μm and 1.625 μm, cores #1 and #4 had larger OH absorption values than cores #2 and #3. According to these results, Rayleigh scattering seems to be one of the loss increase factors in the fabricated 4CF. This is appears to be due to its relatively deep depressed layer. The OH absorption is considered to contribute to the loss difference between the fabricated 4CF and the G.654.B fiber in the short wavelength region. Furthermore, the relatively large OH absorption values of cores #1 and #4 can explain the loss differences among the cores.

Figure 5 shows the measured values of the inter-core XT between neighboring cores throughout the CL-band. The fabricated 4CF was wound on an 80-mm radius fiber bobbin. Conventional SMFs were spliced with the core under test to launch and extract test lights. To prevent the

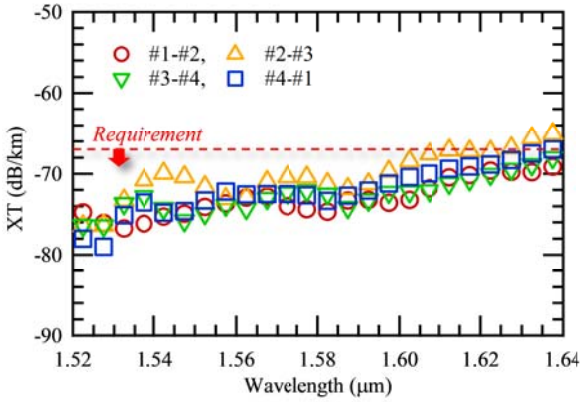

Fig. 5 Measurement results of wavelength dependence of the inter-core XT in the C+L-band

cladding mode at the splicing point from being detected, a 25-km SMF was set between the tested fiber and the photo detector. Red, yellow, green and blue symbols represent the measured values of inter-core XT for core-pairs #1-#2, #2-#3, #3-#4 and #4-#1, respectively. The red broken line indicates our design goal. Inter-core XT increased linearly along with the wavelength in each core pair. Here we confirmed the inter-core XT of lower than -67 dB/km in the C+L-band. These results imply that the total XT is lower than -24 dB at all wavelengths in the C+L-band, even after 10, 000 km propagation. Here, it should be noted that lager bending radius increases the XT which may result in exceeding our requirement for the XT [16]. However, we can expect that the random bending added to the 4CF in the optical fiber cables is not larger as 80 mm or more effectively. Thus, the proposed 4CF is expected to realize 10,000-km transmission systems with 16QAM signaling in the C+L-band.

As seen above, an ultra-low XT 4CF was successfully fabricated within the standard 125-μm diameter cladding while maintaining the optical properties comparable to those of conventional CSFs.

4. Applicability to long-distance transmission systems

Hereinafter, we discuss the applicability of the fabricated 4CF to practical transmission systems. First, we investigated the influence of lateral pressure on the loss and the inter-core XT. A 140-mm radius fiber bobbin with sandpaper (grade P360) was used to load lateral pressure on the 4CF [17]. We controlled the pressure on the tested fiber by fiber winding tension. A conventional SMF transmitted test lights from the laser source to the each core under test in the 4CF through an offset splicing point. To measure the loss under lateral pressure, the micro-bending loss, we utilized OTDR measurements at the wavelength of 1.625 μm and a pulse width of 10 ns. In measuring inter-core XT under the lateral pressure, a lightwave from a wavelength tunable laser diode was

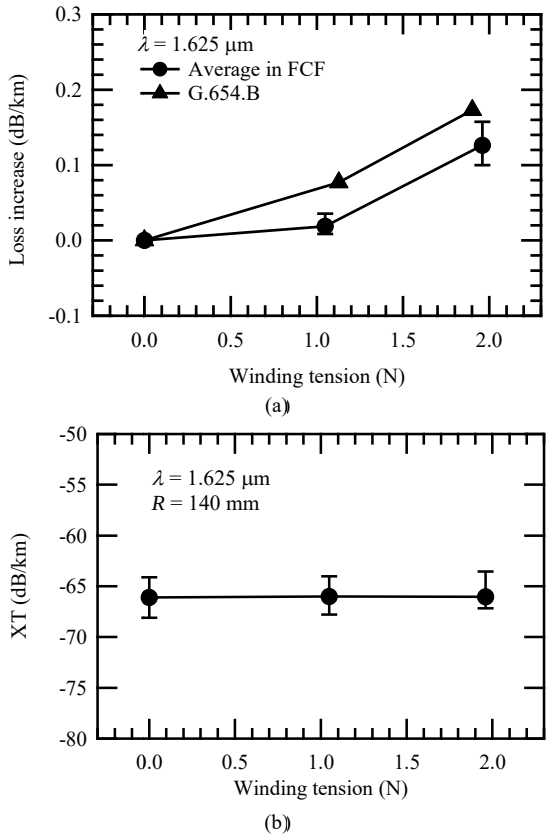

Fig. 6 Winding tension dependence of (a) the loss increase and (b) the inter-core XT at a wavelength of 1.625 μm

launched into one core and a 25-km conventional SMF as used to acquire the results shown in Fig. 5. Figure 6(a) plots the measured loss increase from the loss under a winding tension of 0 N in the fabricated 4CF (0.7-km long) and a conventional G.654.B fiber (0.65-km long) for reference. The plots and the error bars of the fabricated 4CF describe the averaged values and the maximum and minimum values among the cores. The loss increase observed in the G.654.B fiber was 0.17 dB/km at the winding tension of 1.9 N. On the other hand, that in the fabricated 4CF was 0.13 dB/km at the winding tension of 2.0 N. Namely, the fabricated fiber had smaller micro-bending losses than the G.654.B fiber. This is considered to be due to the extremely small α_b of the fabricated 4CF.

Figure 6(b) plots the measured winding tension dependence of the inter-core XT of the fabricated 4CF. The plots and error bars indicate the averaged values and the maximum and minimum values among the cores measured at the wavelength of 1.625 μm. There were no noticeable changes for winding tension values up to 2 N. As is clear, the lateral pressure had sufficiently small influence on the loss and the inter-core XT in the fabricated 4CF. Here, we found the slightly higher XT in fig. 6(b) than that in fig. 5. It can be considered that the larger radius of the fiber bobbin induced the increase of

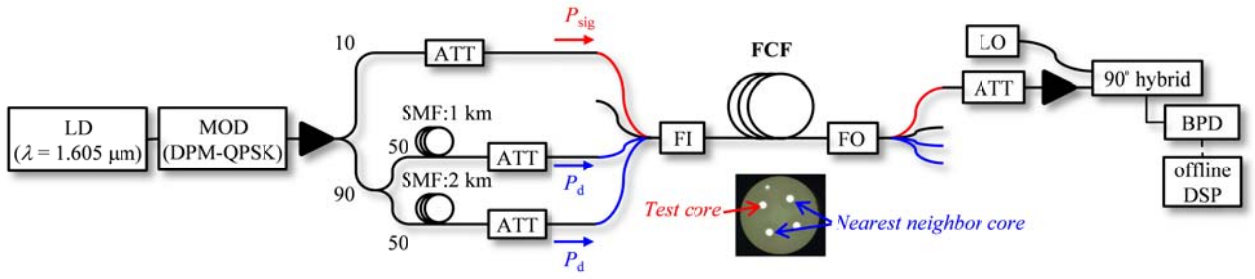

LD: Laser diode, MOD: Modulator, ATT: Attenuator, FI: Fan-in device, FI: Fan-out device, LO: Local Oscillator, BPD: Balanced photo detector

Fig. 7 Transmission experiment setup

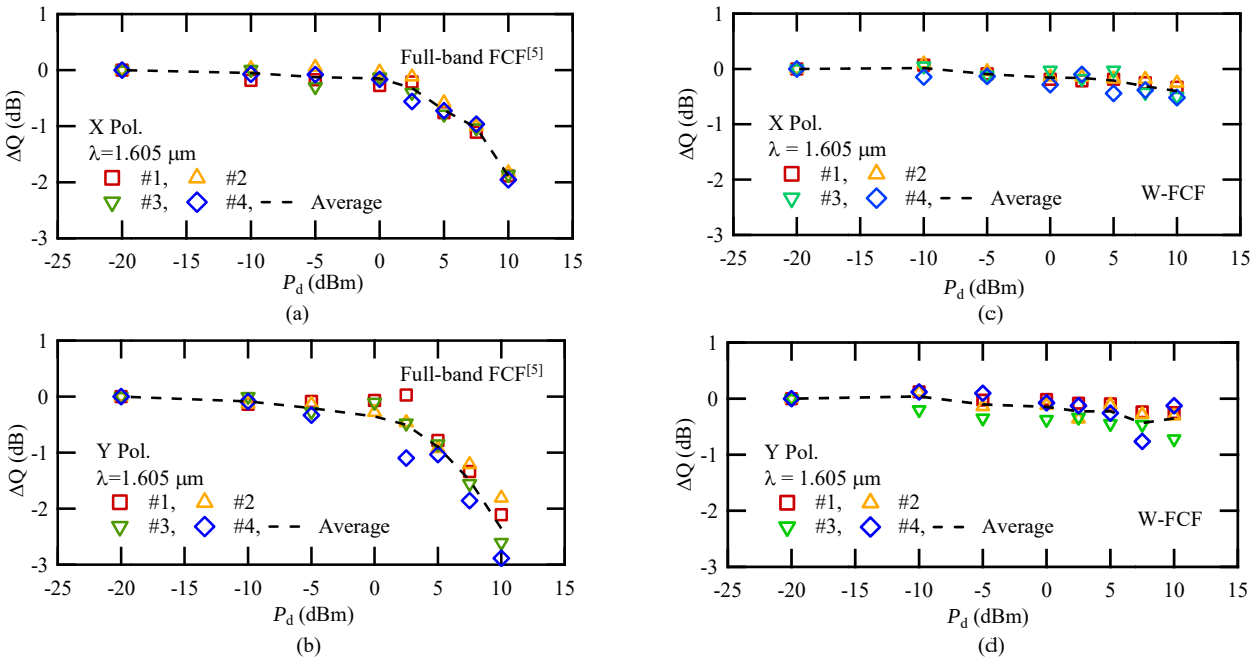

Fig. 8 Measurement results of the inter-core XT influence on the Q-factor in (a, b) the full-band FCF [5] and (c, d) the fabricated FCF

the XT as mentioned previously. These results imply that the fabricated 4CF offers excellent applicability to high density optical fiber cables from the aspect of micro-bending sensitivity.

Next we conducted a transmission experiment to investigate the impact of XT on transmission performance for 10,000-km inter-continental transmission systems. The XT noise for a certain transmission distance was simulated by controlling the transmission power of dummy signals on the neighboring cores. Figure 7 shows the transmission setup. The transmission signals were produced by a laser source (LD) and DP-QPSK 20G-modulator (MOD). The transmission wavelength was 1.605 μm to investigate the worst influence of XT on transmission quality. Signals were divided to the transmission signals and dummy signals by a 10:90 coupler after being amplified by a erbium-doped fiber amplifier (EDFA). For the test core, the optical attenuator (ATT) adjusted the transmission power to -20 dBm. For the cores neighboring the test core, the signals were divided by 50:50 coupler, and launched into 1 km and 2 km standard SMFs to completely eliminate the correlation between each dummy signal and the transmission signal. ATTs in the transmission paths of both dummy signals controlled transmitted power to the range of -20~+10 dBm to simulate the received XT noise at various transmission lengths. A fan-in device (FI) transferred transmission and dummy signals into the test core and its neighboring cores of a 25-km 4CF. A fan-out device (FO) extracted transmitted signals from the test core. Conventional coherent detection was realized using a 90 degree hybrid, local oscillator (LO) and balanced photo detector (BPD). The transmission quality was analyzed by offline digital signal processing (DSP). In this experiment, a 20-km 4CF designed for a full-band transmission was also investigated for comparison [5]. The inter-core XT of the full-band 4CF was -46 dB (average) after 20-km propagation in at λ = 1.605 μm.

Fig. 8(a) and 8(b) show the measured values of the full-band 4CF in X and Y polarization. Each symbol indicates a measured value and the dashed line shows the average values between cores. The vertical axis shows the Q-factor change from the Q-factor at dummy power

of -20 dBm. We confirmed that the transmission quality degraded as the dummy signal power increased. The dummy signal power of 5-dBm degraded the Q-factor by 1 dB. These dummy signals are assumed to impose average XT noise of -18 dB on the test core. Considering this estimated XT noise value, the measured Q-factor degradations are consistent with the investigations of Q-factor dependency on XT in Refs. [14, 15]. Because such XT noise corresponds to that in a 6,300-km transmission system, the tested full-band 4CF is expected to be feasible with such a system transferring DP-QPSK signals at the wavelength of 1.605 μm or less. On the other hand, Fig. 9(c) and 9(d) show the Q-factor change measured in the fabricated 4CF in X and Y polarization. We confirmed an average Q-factor degradation of -0.4 dB even at the dummy signal power of 10 dBm. Considering the inter-core XT measured in Fig. 5, the dummy signals with optical power of 10 dBm imposed average XT noise of -20 dB on the test core. This XT noise corresponds to that after 25,000-km propagation including the FI/FO devices. These experimental results indicate that a Q-factor degradation of less than 1 dB is possible for DP-QPSK transmission over 25,000-km of fabricated 4CF. In case of the full-band 4CF, a Q-factor degradation of -0.4 dB was seen at the dummy power of 0 dBm. Thus we expect that the fabricated 4CF has the potential for a 10-time longer transmission than the full-band 4CF. Generally, a long-distance transmission line has many splicing points and their core-offset and rotational misalignment seem to degrade fiber XT and loss. Therefore, it is important to consider the influence of the splice on the loss and XT besides of the optical characteristics of the 4CF to design of the ultra-long distance MCF transmission line.

4. Conclusion

We proposed an ultra-low XT 4CF with standard 125-μm cladding. Its W-shaped index profile realized the low-XT of less than -67 dB/km at the wavelength of 1.625 μm; its other optical properties are compatible with ITU-T G.654.B fiber. Because we also confirmed adequate micro-bending resistance of the loss and the XT characteristics, the fabricated 4CF is expected to be applicable to high-density optical fiber cables. Transmission experiments indicated that the fabricated 4CF is expected to offer a Q-factor degradation (induced by the inter-core XT) of less than 1 dB even after 25,000-km transmission of DP-QPSK signals. Moreover, we expect that the fabricated 4CF has the potential for 10-times greater transmission length that the full-band 4CF. On the basis of these results, we conclude that the fabricated 4CF with standard 125-μm cladding can realize 10,000-km class, long-distance SDM transmission systems.

References

[1]. D. Soma *et al*., “10.16 Peta-bit/s Dense SDM/WDM transmission over Low-DMD 6-Mode 19-Core Fibre Across C+L Band,” *2017 European Conference on Optical Communication (ECOC)*, Gothenburg, pp. 1-3 (2017).

[2]. B. J. Puttnam *et al*., "2.15 Pb/s transmission using a 22 core homogeneous single-mode multi-core fiber and wideband optical comb," *2015 European Conference on Optical Communication (ECOC)*, Valencia, 2015, pp. 1-3.

[3]. M. Koshiba *et al*., “Heterogeneous multi-core fibers: proposal and design principle,” *IEICE Electronics Express*, 6, 2, pp. 98-103 (2009)

[4]. Y. Sasaki *et al*., “Single-mode 37-core fiber with a cladding diameter of 248 μm,” *2017 Optical Fiber Communications Conference and Exhibition (OFC)*, Los Angeles, CA, pp. 1-3 (2017).

[5]. T. Matsui *et al*., “Design of 125 μm cladding multi-core fiber with full-band compatibility to conventional single-mode fiber,” *2015 European Conference on Optical Communication (ECOC)*, Valencia, pp. 1-3 (2015).

[6]. T. Gonda *et al*., “125 μm 5-core fibre with heterogeneous design suitable for migration from single-core system to multi-core system,” *2016 European Conference on Optical Communication (ECOC)*, Dusseldorf, Germany, pp. 1-3 (2016).

[7]. T. Tsuritani *et al*., “Field Test of Installed High-Density Optical Fiber Cable with Multi-Core Fibers toward Practical Deployment,” *2019 Optical Fiber Communications Conference and Exhibition (OFC)*, San Diego, CA, USA, pp. 1-3 (2019).

[8]. T. Hayashi *et al*., “Field-Deployed Multi-Core Fiber Testbed,” *2019 24th OptoElectronics and Communications Conference (OECC) and 2019 International Conference on Photonics in Switching and Computing (PSC)*, Fukuoka, Japan, pp. 1-3 (2019).

[9]. T. Matsui *et al*., “118.5 Tbit/s transmission over 316 km-long multi-core fiber with standard cladding diameter,” *2017 Opto-Electronics and Communications Conference (OECC) and Photonics Global Conference (PGC)*, Singapore, pp. 1-2 (2017).

[10]. Y. Tamura *et al*, “Low-Loss Uncoupled Two-Core Fiber for Power Efficient Practical Submarine Transmission,” *2019 Optical Fiber Communications Conference and Exhibition (OFC)*, San Diego, CA, USA, pp. 1-3 (2019).

[11]. Y. Sagae *et al*., “Ultra-Low-XT Multi-Core Fiber with Standard 125-μm Cladding for Long-Haul Transmission,” *2019 24th OptoElectronics and Communications Conference (OECC) and 2019 International Conference on Photonics in Switching and Computing (PSC)*, Fukuoka, Japan, pp. 1-3 (2019).

[12]. S. Makovejs *et al*., “Towards Superior Transmission Performance in Submarine Systems: Leveraging UltraLow Attenuation and Large Effective Area,” *Journal of Lightwave Technology*, 34, pp. 114-120 (2016).

[13]. M. Tsukitani *et al*., "Ultra Low Nonlinearity Pure-Silica-Core Fiber with an Effective Area of 211 μm^2 and Transmission Loss of 0.159dB/km," *2002 European Conference on Optical Communication (ECOC)*, Copenhagen, pp. 1-2 (2002).

[14]. P. J. Winzer *et al*., "Penalties from In-Band Crosstalk for Advanced Optical Modulation Formats," *2011 European Conference and Exposition on Optical Communications*, Geneva, pp. 1-3 (2011).

[15]. T. Hayashi *et al*., "Behavior of Inter-Core Crosstalk as a Noise and Its Effect on Q-factor in Multi-Core Fiber," *IEICE TRANSACTIONS on Communications,* E97-B, 5, pp.936-944 (2014).

[16]. M. Koshiba *et al*., "Analytical Expression of Average Power-Coupling Coefficients for Estimating Intercore Crosstalk in Multicore Fibers," *IEEE Photonics. Journal*, 4, 5, pp. 1987-1995 (2012).

[17]. IEC, "Optical fibres – Measurement methods – Microbending sensitivity," TR 62221 (2001).

Yuto Sagae received B.E. and M.E. degrees from Tohoku University, Miyagi, Japan, in 2013 and 2015, respectively. In 2015, he joined NTT Access Network Service Systems Laboratories, NTT, Ibaraki, Japan, where he has been researching optical fiber designs. Mr. Sagae is a member of the Institute of Electronics, Information and Communication Engineers. Mr. Sagae was a recipient of the 24th OptoElectronics and Communications Conference / International Conference on Photonics In Switching and Computing 2019 (OECC/PSC 2019) Best Paper Award in 2019.

Takashi Matsui received B.E., M.E. and Ph. D. degrees in electronic engineering from Hokkaido University, Sapporo, Japan, in 2001, 2003 and 2008, respectively. He also attained the status of Professional Engineer (P.E.Jp) in electrical and electronic engineering in 2009. In 2003, He joined NTT Access Network Service Systems Laboratories, Ibaraki, Japan. He has been engaged in research on optical fiber design and measurement.
Dr. Matsui is a member of the Institute of Electronics, Information and Communication Engineers (IEICE) of Japan. He received the Young Researcher's Award from the IEICE in 2008 and METI international standardization encourage award in 2014.

Taiji Sakamoto received B.E., M.E. and Ph.D. degrees in electrical engineering from Osaka Prefecture University, Osaka, Japan, in 2004, 2006 and 2012, respectively. In 2006, he joined NTT Access Network Service Systems Laboratories, NTT, Ibaraki, Japan, where he has been engaged in research on optical fiber nonlinear effects, low nonlinear optical fiber, few-mode fiber, and multi-core fiber for optical MIMO transmission systems. Dr. Sakamoto is a member of the Institute of Electronics, Information and Communication Engineers.

Kazuhide Nakajima received M.S. and Ph.D. degrees in electrical engineering from Nihon University, Chiba, Japan, in 1994 and 2005, respectively. In 1994, he joined NTT Access Network Systems Laboratories, Tokai, Ibaraki, Japan, where he engaged in research on optical fiber design and related measurement techniques. He is currently a Group Leader (Senior Distinguished Researcher) of NTT Access Network Service Systems Laboratories, Tsukuba, Ibaraki, Japan. Dr. Nakajima is acting as a Rapporteur of Q5/SG15 of ITU-T since 2009. He is a member of the Institute of Electrical and Electronics Engineers (IEEE), the Optical Society (OSA), the Institute of Electronics, Information and Communication Engineers (IEICE) of Japan and the Japan society of applied physics (JSAP). He received the best paper award in OECC'96, the best paper award in IEICE'11, the achievement award in IEICE'12, and Maejima Hisoka award in 2016.